

Oxidation of arsenite by self-regenerative bioactive birnessite in a continuous flow column reactor

Nishi, Ryohei

Department of Earth Resources Engineering, Faculty of Engineering, Kyushu University

Kitjanukit, Santisak

Department of Earth Resources Engineering, Faculty of Engineering, Kyushu University

Nonaka, Kohei

Department of Earth Resources Engineering, Faculty of Engineering, Kyushu University

Okibe, Naoko

Department of Earth Resources Engineering, Faculty of Engineering, Kyushu University

<https://hdl.handle.net/2324/4739237>

出版情報 : Hydrometallurgy. 196 (105416), 2020-09. Elsevier

バージョン :

権利関係 :



Hydrometallurgy (IBS2019 Special Issue)

Title: Oxidation of arsenite by self-regenerative bioactive birnessite in a continuous flow column reactor

Ryohei Nishi, Santisak Kitjanukit, Kohei Nonaka and Naoko Okibe*

Department of Earth Resources Engineering, Faculty of Engineering, Kyushu University, 744 Motoooka,
Nishi-ku, Fukuoka 819-0395, Japan

*Corresponding author

Tel. and Fax: +81 92 802 3312

E-mail address: okibe@mine.kyushu-u.ac.jp (Naoko OKIBE)

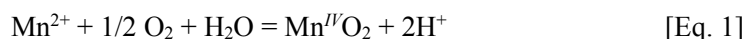
Keywords: arsenite; oxidation; birnessite, Mn-oxidizing bacteria, continuous column reactor

Abstract

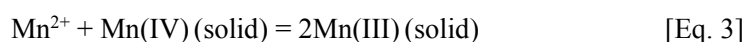
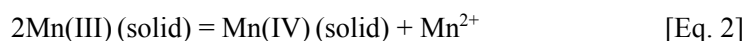
Naturally occurring manganese (Mn) oxide, biogenic birnessite $((\text{Na}, \text{Ca}, \text{K})_{0.5} \text{Mn}^{\text{III}, \text{IV}}_2\text{O}_4 \cdot 1.5 \text{H}_2\text{O})$, is involved in the geochemical cycling of variety of metals including arsenic (As). This natural reaction was exploited in this study to develop a sustainable oxidation treatment process of As(III) to the less soluble (and less toxic) As(V). It is known that the birnessite surface becomes passivated during As(III) oxidation, which quickly decreases its reactivity. The cycle batch test and the following XANES (X-ray absorption near-edge structure) analysis in this study confirmed that combining chemical As(III) oxidation by birnessite with simultaneous birnessite regeneration by Mn-oxidizing microorganisms (*Pseudomonas* sp. SK3) can avoid passivation of Mn^{III} -precipitates and enables continuous As(III) oxidation while increasing the AOS (average oxidation state) of birnessite. This chemical/microbiological synergism was observed for the As(III) concentration range of 0.2-0.5 mM with 0.1% birnessite, wherein no net Mn loss from birnessite was noticed for complete As(III) oxidation. The continuous column test was run for 40 days at a HRT (hydraulic retention time) of 3 hours by feeding a 0.2 mM As(III) solution. The As(III) oxidation efficiency of > 98% was consistently achieved while strictly controlling the Mn^{2+} dissolution throughout the test period. This study concluded that by taking advantage of a robust microbial Mn-oxidizing activity, the use of “bioactive” birnessite realizes self-sustainable oxidation of As(III), without necessitating additional feed of oxidant birnessite, Mn^{2+} ions or organics.

Introduction

Mn-oxides are known as naturally occurring oxidizing agents involved in a variety of redox reactions of organic/inorganic species and compounds in the environment. Natural Mn-oxides found in circumneutral pH environments are often poorly crystalline and considered to be of a biological origin (primarily phyllomanganate most similar to δ -MnO₂ or acid birnessite; Tebo et al., 2004). Microbiological Mn²⁺ oxidation also follows the stoichiometry of chemical reaction represented as [Eq. 1], which is typically catalyzed by multicopper oxidase enzymes of Mn-oxidizing bacteria via two sequential one-electron transfer (Mn²⁺ → Mn(III) → Mn(IV); Tebo et al., 2004):



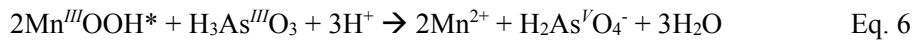
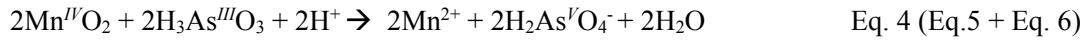
Abiotic Mn²⁺ oxidation was also reported to occur in a two-step process, in which Mn^{III}-oxides/oxyhydroxides (such as hausmannite (Mn^{II, III}₃O₄) and feitknechtite (β-Mn^{III}OOH)) are initially formed, followed by slower disproportionation reactions, eventually forming Mn^{IV}O₂ (rate-limiting step favoring pH <9; [Eq. 2]). Whilst Mn^{III} is effectively stabilized by the comproportionation of Mn²⁺ and Mn^{IV} in alkaline conditions (Murray et al., 1985; Tebo et al., 2004; Takashima et al., 2011; [Eq. 3]).



Regardless of the origin (biotic or abiotic) of Mn-oxides, geochemical cycling of a variety of metals on the Earth's crust is also affected by the action of such naturally occurring oxidants (Fendorf and Zasoski, 1992; Manceau et al., 1997). The involvement of Mn-oxides in the oxidation of As(III) gives especially a critical indication that can dictate the fate of this highly toxic metal in the environment.

Arsenic contamination in groundwater and other aquatic systems is widely reported across the world, with its concentration ranging up to around 50 mg/L As (Singh et al., 2015). Inorganic As species are solubilized typically in the form of arsenite (H₃As^{III}O₃) or arsenate (H₃As^VO₄), with the former more toxic and soluble. The treatment of As(III)-polluted waters thus often employs the oxidation step of As(III) to less toxic/soluble As(V) form. A variety of methodologies proposed for As(III) oxidation range from the use of conventional chemical oxidants (i.e., Cl₂, O₃, H₂O₂) to photochemical/photocatalytic and biological oxidation (Sorlini et al., 2010; Singh et al., 2015; Okibe et al., 2014; Tanaka and Okibe, 2018; Okibe and Fukano, 2019). The use of Mn-oxides is also one of the approaches studied for the purpose of As(III) oxidation [Eq. 4], and it is known that their reactivity can vary based on their mineralogy (Oscarson et al., 1983). A number of studies reported the As(III) oxidizing ability of phyllomanganates. However, it is well documented that the reactivity of phyllomanganates declines over time owing to secondary mineral

passivation (Scott et al., 1995; Manning et al., 2002; Tournassat et al., 2002). Mn^{III}-intermediates (Mn^{III}OOH*) were detected during the As(III) oxidation to passivate the surface of phyllomanganates ([Eq. 5], [Eq. 6]; Nesbitt et al., 1998; Lafferty et al., 2010a; 2010b]:



It was also suggested that most of the resultant As(V) anions produced by [Eq. 4] are released into solution, while some may remain on the mineral surface by adsorption, thus contributing to the passivation of phyllomanganates. Formation of Mn-As precipitates was also suggested to become a cause of the mineral passivation under certain conditions (Manning et al., 2002; Tournassat et al., 2002).

In order to overcome the above passivation problems and to maintain the prolonged oxidant reactivity, the introduction of microbial Mn-oxidizing ability in this reaction may represent one of the solutions. Watanabe et al. (2013) utilized fungal biogenic manganese oxides (BMOs) in a batch study and underlined the importance of its self-regeneration to maintain the As(III) oxidation reaction. Katsoyiannis et al. (2004) suggested the effectiveness of indigenous Mn- and Fe-oxidizing bacterial consortium for the oxidative removal of As(III) from groundwater contaminated with low-level As, Mn and Fe ions. The authors reported the occurrence of the following sequential reactions in the continuous column treatment system: (i) microbial oxidation of Mn²⁺ to Mn(IV) and Fe²⁺ to Fe³⁺, (ii) microbial oxidation of As(III) to As(V), (iii) precipitation of Mn^{IV}-oxides, (iv) abiotic oxidation of As(III) by Mn^{IV}-oxides, and (e) As(V) adsorption on Mn^{IV}-oxides.

Theoretically, if the reductively-dissolved Mn²⁺ after As(III) oxidation (according to [Eq. 6]) could be simultaneously re-oxidized back to Mn-oxides by Mn-oxidizing bacteria based on [Eq. 1], the As(III) oxidation reaction would continue sustainably without consuming originally-provided oxidant (i.e., without necessitating additional Mn²⁺ inflow). To our knowledge, such a self-sustainable (free of Mn²⁺ inflow), continuous column process for the As(III) oxidation using biogenic birnessite is yet unknown. Therefore, this study aimed to develop a new As(III)-oxidation treatment process targeting relatively high-level As contamination in groundwater (i.e., dozens of ppm), by combining the robust bacterial Mn-oxidizing ability for continuous regeneration of the oxidant birnessite.

2. Materials and Methods

2.1 Microorganism

Mn-oxidizing bacterium, *Pseudomonas* sp. strain SK3 isolated from a metal-refinery wastewater treatment system (Kitjanukit et al. 2019) was routinely sub-cultured and maintained in half-strength lysogeny broth (LB) medium (0.5% (w/v) NaCl; 0.5% (w/v) tryptone; 0.25% (w/v) yeast extract) in Erlenmeyer flasks (shaken at 120 rpm, 25°C). Cells were pre-grown overnight, collected and washed with 0.8% (w/v) NaCl solution prior to use in the following Mn oxidation tests.

2.2 Preparation of biogenic birnessite

Pseudomonas sp. SK3 was inoculated in 1 L of peptone–yeast extract–glucose-1 (PYG-1) medium (0.025% peptone; 0.025% yeast extract; 1 mM glucose; 2.02 mM MgSO₄•7H₂O; 0.068 mM CaCl₂•2H₂O; 4.5 g/L PIPES (piperazine-N,N'-bis(2-ethanesulfonic acid); pH 7.0 with NaOH) containing 100 mg/L Mn²⁺ (as MnSO₄) and 3 μM Cu²⁺ (as CuCl₂) (in 2 L Erlenmeyer flasks). After incubation (shaken at 120 rpm, 25°C) for 96 hours, black birnessite precipitates were collected, washed with 0.8% NaCl solution and then freeze-dried overnight prior to use in section 2.3.

2.3 As(III)-oxidation test (cycle flask batch test)

Biogenic birnessite (prepared in section 2.2) was added to a pulp density of 0.1% (w/v) into 100 mL Erlenmeyer flasks containing 50 mL of PYG-2 medium (0.01% peptone; 0.01% yeast extract; 1 mM glucose; 2.02 mM MgSO₄•7H₂O; 0.068 mM CaCl₂•2H₂O; 4.5 g/L; pH 7.0 with NaOH) containing 3 μM Cu²⁺. The initial As(III) concentration was set to 0.2 mM (added as NaAsO₂). In order to evaluate the effect of active Mn-oxidizing cells in the system, tests were set up with and without pre-grown *Pseudomonas* sp. SK3 cells (10⁹ cells/mL). Birnessite-free controls containing only SK3 cells (10⁹ cells/mL) were also set up in parallel. The flasks were incubated shaken at 120 rpm, 25°C for 24 hours, followed by centrifugation to replace the supernatant with the same fresh medium. This procedure was repeated three times. All tests were conducted in duplicate flasks. Samples were withdrawn regularly to monitor pH, Eh (vs. SHE), planktonic cell density, As(III) concentration (molybdenum blue method; Blomqvist et al., 1993; Murphy and Riley, 1962) and total Mn and As concentrations (ICP-OES; Optima8300, Perkin Elmer). Precipitates were collected after the 1st- and 3rd-cycles (at 24 and 72 hours) and freeze-dried overnight for X-ray diffraction (XRD) (Ultima IV, Rigaku; Cu Kα 40 mA, 40 kV) and X-ray absorption near-edge structure (XANES) analyses.

Additionally, the effect of different initial As(III) concentrations (0.2-0.7 mM) was compared in a single batch test to evaluate the robustness of this microbially-catalyzed coupling reaction at higher As toxicity levels.

2.4 X-ray absorption near-edge structure (XANES)

Biogenic birnessite samples (collected in section 2.3) were quantitatively mixed with boron nitride and pressed into a tablet. The Mn K-edge spectra were collected (transmission mode; 6200-8500 eV) at SAGA-LS (1.4 GeV, 75.6 m; Kyushu University Beam Line 06). Average Mn oxidation state (AOS) of biogenic birnessite was calculated based on the linear combination fitting of Mn K-edge XANES spectra (6200-6600 eV) using the Athena program (Demeter version 0.9.24).

2.5 Comparison of As(III)-oxidizing reactivity of $\text{Mn}^{\text{IV}}\text{O}_2$ and $\text{Mn}^{\text{III}}_2\text{O}_3$ (chemical reagents)

MnO_2 (Wako; 138-09675) or Mn_2O_3 (Kojundo chemical laboratory; 215558) was added to a pulp density of 0.15 % into 100 mL Erlenmeyer flasks containing 50 mL of PIPES solution (4.5 g/L; pH 7.0 with NaOH) containing 1.8 mM As(III). The flasks were incubated shaken at 120 rpm, 25°C. Samples were withdrawn to monitor As(III) and total Mn concentrations.

2.6 Continuous As(III)-oxidation column test

Natural zeolite from Shimane, Japan (No.5, 0.5-1.5 mm, Shinsei Corporation; 68% SiO_2 , 12% Al_2O_3 , 2.5% Na_2O , 1.9% K_2O , 1.7% CaO ; specific surface area 246 m^2/g) was used as supporting material for biogenic birnessite and Mn-oxidizing bacterial cells ("Bio-zeolite"). Bio-zeolite was prepared as follows: *Pseudomonas* sp. SK3 cells (at a density of 10^9 cells/mL) and 50 g zeolite particles were added into 1 L of PYG-1 medium (pH 7.0 with NaOH; 2 L Erlenmeyer flasks) containing 100 mg/L Mn^{2+} and 3 μM Cu^{2+} . After 96-hour incubation (at 120 rpm, 25°C), the supernatant was discarded by decantation and replaced with the same fresh medium. This was repeated three times and the products were packed into the column. The first column run was carried out while altering the HRT from 12 hours to 2 hours to look for the optimal speed. For the second column run, the HRT was fixed at 3 hours. Synthetic As(III)-polluted water used as feedwater contained 2.02 mM $\text{MgSO}_4 \cdot 7\text{H}_2\text{O}$, 0.068 mM $\text{CaCl}_2 \cdot 2\text{H}_2\text{O}$, 4.5 g/L PIPES, 3 μM Cu^{2+} and 0.2 or 0.4 mM As(III); pH 7.0 with NaOH). PIPES was removed from the feed water on day 27 to eliminate any artificial buffering effect. Liquid samples were regularly withdrawn from the inlet/outlet of the column to monitor pH, Eh (vs. SHE) and the concentration of As(III), total Mn and total As.

3. Results and discussion

3.1 Mn-oxidizing bacteria simultaneously regenerate birnessite during the chemical As(III) oxidation by birnessite

At first, in order to clarify the capability of real-time Mn oxidation by *Pseudomonas* sp. SK3 during the chemical oxidation of highly toxic As(III) by birnessite, tests were set up with or without the presence of active cells. Freeze-dried biogenic birnessite was added only once at 0.1% before initiating the 1st-cycle, and neither additional birnessite nor any form of Mn was supplemented thereafter. The absence of microbial As(III)-oxidizing ability was confirmed as a premise (Fig. 1a, b).

According to [Eq. 4], the initial dose of 0.1% biogenic birnessite is calculated to be over 20-folds of the stoichiometric amount required for complete oxidation of 0.2 mM As(III) (approx. 86% of Mn in biogenic birnessite used in this test exists as Mn(IV)). Under the abiotic condition, however, this excess birnessite oxidized only 63% of As(III) during the 1st-cycle (Fig. 1a), accompanied by a release of 0.4 mM Mn^{2+} (9% of Mn lost from the initially added biogenic birnessite). Since fresh biogenic birnessite contain some adsorbed Mn^{2+} ions (Santisak et al. 2019), the released Mn^{2+} in the 1st-cycle is comprised of some desorbed Mn^{2+} ions plus reductively-dissolved Mn^{2+} ions (Fig. 1c, d). The 1st-cycle in the abiotic condition was followed by increasingly weaker As(III) oxidation in the 2nd- and 3rd-cycles (Fig. 1a). Mn^{2+} dissolution continued and the amount of Mn lost from the initial birnessite dose became 19% by the end of the 3rd cycle (Fig. 1d).

In contrast, the presence of active Mn-oxidizing cells led to complete oxidation of 0.2 mM As(III) within 24 hours in the 1st-cycle (Fig. 1a). Despite that the net amount of birnessite was constant throughout the cycle test (unless dissolved), the As(III) oxidation speed in the biotic condition became even higher in the following 2nd- and 3rd-cycles (As(III) oxidation completed within 6 hours; Fig. 1a) and Mn^{2+} dissolution was negligible (Fig. 1c, d).

Under conditions where As(III) oxidation was proceeded (birnessite \pm cells), a small portion of the total soluble As was immobilized in each cycle, especially at later cycles (Fig. 1b). This is likely due to the adsorption of the resultant As(V) on the birnessite surface, which was reported to occur at crystallite edges and interlayer domains (Manning et al., 2002). Formation of Mn-As precipitates was unlikely in this study since ion concentrations were far below its K_{sp} (Schacht and Ginder-Vogel, 2018; Tournassat et al., 2002; Sadiq, 1997). The reason for a slightly increased As(V) adsorption at later cycles (Fig. 1b) may be attributed to the As(III) oxidation reaction causing a surface alteration to create fresh reaction sites for As(V) on birnessite surfaces (Manning et al., 2002). A slightly less As(V) adsorption in 1st- and 2nd-cycles in the birnessite + cells condition than in the cell-free counterpart may have been caused by any organic passivation on the mineral surface; however, this trend was reversed in the 3rd-cycle, possibly because

continuously extensive As(III) oxidation in the biotic system more readily created As(V) adsorption sites (Manning et al., 2002). Although Parikh et al. (2010) reported the negative influence of bacteria/biopolymer coatings on the initial As(III) oxidation kinetics by δ -MnO₂, this study showed that the advantage of microbial Mn-oxidizing activity was far greater than the possible passivation effect caused by their biomass.

3.2 The average oxidation state (AOS) of birnessite increases through its dissolution-recrystallization process mediated by Mn-oxidizing bacteria

The reasons for the increased As(III) oxidation efficiency during the cycle batch test in biotic conditions (section 3.1) were investigated by XANES and XRD analyses. The AOS of biogenic birnessite before starting the cycle As(III) oxidation test (at 0 hours) was 3.80 (Mn^{IV} 86.1%; Mn^{III} 7.4%; Mn^{II} 6.5%), which then gradually decreased down to 3.69 (Mn^{IV} 78.2%; Mn^{III} 12.1%; Mn^{II} 9.7%) after 3 cycles in the abiotic condition (Fig. 2). The trend was reversed in the biotic condition and the AOS increased up to 3.94 (Mn^{IV} 95.2%; Mn^{III} 3.6%; Mn^{II} 1.2%) after 3 cycles (Fig. 2).

The XRD results indicated no evidence of improved birnessite crystallinity during the cycle test, and no apparent difference in the XRD peaks was found between the abiotic and biotic conditions (Supplemental Fig. 1). Another possible reason for the improved As(III) oxidation rate during the cycle test in the biotic condition can be attributed to the cell density in the system: Whilst the planktonic cell density was mostly stable (at $6\text{--}8 \times 10^8$ cell/mL in all cycles), sessile/trapped cells on the birnessite surface may have increased during the microbial birnessite regeneration process, eventually improving the As(III) oxidation rate.

Decreased As(III) oxidation rate (Fig. 1a) accompanied by the lowered Mn AOS (Fig. 2) in the abiotic condition can be explained by passivation of the birnessite surface with Mn^{III}-products formed during As(III) oxidation by birnessite [Eq. 5, 6] as well as through comproportionation reaction [Eq. 3]. This observation was not evidenced by the XRD analysis (Supplemental Fig. 1), since such Mn^{III}-intermediates are likely poorly crystalline. A separate test compared the reactivity of Mn(VI) and Mn(III) towards As(III) oxidation (by using reagent-grade crystalline Mn^{III}₂O₃ and α -Mn^{IV}O₂). As shown in Fig. 3, As(III) oxidation by Mn(III) was much weaker than that by Mn(IV), supporting the correlation between the decreased As(III) oxidation rate and the lowered Mn AOS.

The results from 3.1 and 3.2 confirmed that the combination of chemical As(III) oxidation by birnessite and microbial birnessite regeneration by Mn-oxidizing bacteria enables self-sustainable As(III) oxidation reaction. This effective synergism was seen for the initial As(III) concentration range of 0.2–0.5 mM (Fig. 4): Within this range, the molar ratio of [Mn²⁺ released]/[As(III) oxidized] (Mn/As ratio) at the very beginning was 1–2 (Fig. 4c), reflecting the spontaneous chemical As(III) oxidation according to Eq. 4 together with some desorbed Mn²⁺ ions from the birnessite structure. The Mn/As ratio then quickly shifted

to negative owing to microbial birnessite regeneration, with its speed affected by the toxic As(III) level (Fig. 4c). There was no net Mn loss from birnessite for completion of As(III) oxidation (Fig. 4b). On the other hand, at the highest initial As(III) concentration of 0.7 mM, a significant amount of Mn^{2+} was released (Fig. 4b) due to deactivation of Mn-oxidizing ability by elevated As(III) toxicity and the As(III) oxidation was not completed (Fig. 4a).

3.3 Continuous self-regenerative bio-zeolite column can process As(III) oxidation at > 98% efficiency

Following the above batch tests, the continuous As(III) oxidation column was set up, as shown in Fig. 5. Firstly, a suitable HRT range was searched at 0.2 mM As(III). As shown in Fig. 6a, high As(III) oxidation efficiencies (94-100%) were observed at HRT from 12 hours to 4 hours. However, soon after the HRT shortened to 2 hours, Mn^{2+} started to dissolve from bio-zeolite and the column efficiency progressively deteriorated; dissolution of only a few percent of Mn from bio-zeolite was shown to seriously worsen the column performance (Fig. 6a). This observation reconfirmed the importance of active Mn-oxidizing bacteria in the system to strictly control the regeneration of birnessite in the column. Except for temporal sorption of a slight amount of As(V) at the beginning, no clear evidence of As(V) sorption was seen, since total As concentrations at the inlet and outlet were nearly identical throughout the column run (Fig. 6b). This observation suggests that birnessite in the column was also free from major passivation via As(V) sorption.

The next column test was conducted at the fixed HRT of 3 hours (Fig. 7) at 0.2 mM As(III) for 40 days. Although *Pseudomonas* sp. SK3 used in this test is a heterotrophic Mn-oxidizer (Kitjanukit et al. 2019), the column test was run without any additional organic sources. For the 40-days-long test period, high As(III) oxidation efficiencies (> 98%) were maintained (Fig. 7a) with strictly controlled Mn^{2+} dissolution (< 0.006 mM; 0.33 mg/L; Fig. 7b) through robust birnessite regeneration by Mn-oxidizing cells. Although there was some pH fluctuation observed after removing the buffering agent PIPES on day 27 (Fig. 7b), the trends of As(III) oxidation and Mn^{2+} dissolution were unaffected (Fig. 7). It can be postulated that the growth of heterotrophic Mn-oxidizing cells relied upon organic substances deriving from their own cell lysates/exudates. This self-sustainable feeding cycle may have proceeded via toxicity of As(III), which possibly accelerated cell regenerations in turn. It is, however, possible that some organics needs to be externally injected to the system at some point, if the column was to run for a much longer period.

In abiotic stirred-flow reactor studies by Lafferty et al. (2010a, b), oxidation of 0.1 mM As(III) by $\delta\text{-MnO}_2$ initially proceeded rapidly but slowed down considerably within several hours, due to passivation of $\delta\text{-MnO}_2$ by Mn^{III} -precipitates (as a result of comproportionations of sorbed Mn^{2+} and Mn(IV) [Eq. 3], rather than Mn(IV) reduction by As(III) [Eq. 4]) as well as by sorption of Mn^{2+} and As(V).

On the other hand, our column reactor packed with “bioactive” birnessite-coated zeolite maintained its high reactivity for over 40 days. The results obtained in the cycle batch test (section 3.1, 3.2) explain the underlying mechanism in the column; robust real-time regeneration of birnessite by active Mn-oxidizing cells strictly controlled the Mn^{2+} dissolution and avoided accumulation of Mn^{III} -precipitates. The AOS of birnessite was likely continuously increased during the column run. There might have been some inhibitory effect of As(V) adsorption onto the birnessite surface due to the presence of cells, as was reported in a study by Jones et al. (2012), wherein the presence of As(III)-oxidizing soil bacteria synergistically improved the As(III) oxidation rate by δ - MnO_2 , but lowered the amount of As(V) adsorption on the mineral surface. Katsoyiannis et al. (2004) reported the improved As(III) oxidation rate by synergism between Mn-oxide and indigenous Mn- and Fe-oxidizing bacteria for the treatment of groundwater containing both low-level As(III) (35 $\mu\text{g/L}$) and Mn^{2+} (0.6 mg/L). This study demonstrated that by employing a robust Mn-oxidizing species, bioactive birnessite is capable of continuous, self-sustainable oxidation of high-level As(III) contaminants in groundwater without even necessitating additional feed of oxidant, Mn^{2+} , or organics, via simultaneous regeneration of the oxidant birnessite while avoiding mineral passivation.

4. Conclusions

- Highly toxic As(III) was chemically oxidized to less toxic/soluble As(V) by biogenic birnessite, while the reaction was incomplete and the reactivity rapidly deteriorated during the cycle batch test.
- The synergism between chemical As(III) oxidation by birnessite and simultaneous birnessite regeneration by Mn-oxidizing *Pseudomonas* SK3 cells enabled complete oxidation of As(III), and the oxidation rate increased during the cycle batch test.
- The XANES analysis suggested that passivation of the birnessite surface with Mn^{III}-mineral caused the declined reactivity in abiotic conditions (birnessite AOS decreased from 3.8 to 3.69 during the cycle batch test), while the improved As(III) oxidation rate in the biotic counterpart corresponded to the increased birnessite AOS from 3.8 to 3.94.
- The above chemical/microbial synergism was effective for the As(III) concentration range of 0.2-0.5 mM in the presence of 0.1% birnessite, where no net Mn loss from birnessite was noticed for complete As(III) oxidation.
- The continuous column test showed the As(III) oxidation efficiency of > 98% throughout the 40 days experiment at the HRT of 3 hours using 0.2 mM As(III) solution, wherein Mn²⁺ dissolution was negligible.
- By employing a robust Mn-oxidizing bacterial species, bioactive birnessite enabled continuous, self-sustainable oxidation of As(III) without necessitating additional feed of oxidant, Mn²⁺, or organics, via simultaneous regeneration of birnessite while avoiding the mineral passivation with Mn^{III}-precipitates or adsorbed As(V) ions.

294 **Acknowledgment**

295 The XAFS experiment was performed at the SAGA Light Source (Kyushu University Beam Line; BL06,
296 No.2019IHK007). This work was partly supported by Japan Oil, Gas and Metals National Corporation
297 (JOGMEC).

298

Reference

Blomqvist, S., Hjellström, K., Sjösten, A., 1993. Interference from arsenate, fluoride and silicate when determining phosphate in water by the phosphoantimonyl molybdenum blue method. *Int. J. Environ. Anal. Chem.* 54, 31-43. <https://doi.org/10.1080/03067319308044425>.

Fendorf, S.E., Zasoski, R.J., 1992. Chromium(III) oxidation by δ -MnO₂. 1. Characterization. *Environ. Sci. Technol.* 26, 79-85. <https://doi.org/10.1021/es00025a006>.

Jones, L.C., Lafferty, B.J., Sparks, D.L., 2012. Additive and competitive effects of bacteria and Mn oxides on arsenite oxidation kinetics. *Environ. Sci. Technol.* 46, 6548-6555. <https://doi.org/10.1021/es204252f>.

Katsoyiannis, I.A., Zouboulis, A.I., Jekel, M., 2004. Kinetics of bacterial As(III) oxidation and subsequent As(V) removal by sorption onto biogenic manganese oxides during groundwater treatment. *Ind. Eng. Chem. Res.* 43, 486-493. <https://doi.org/10.1021/ie030525a>.

Kitjanukit, S., Takamatsu, K., Okibe, N., 2019. Natural attenuation of Mn(II) in metal refinery wastewater: microbial community structure analysis and isolation of a new Mn(II)-oxidizing bacterium *Pseudomonas* sp. SK3. *Water* 11, 507. <https://doi.org/10.3390/w11030507>.

Lafferty, B.J., Ginder-Vogel, M., Sparks, D.L., 2010a. Arsenite oxidation by a poorly crystalline manganese-oxide 1. Stirred-flow experiments. *Environ. Sci. Technol.* 44, 8460-8466. <https://doi.org/10.1021/es102013p>.

Lafferty, B.J., Ginder-Vogel, M., Zhu, M., Livi, K.J.T., Sparks, D.L., 2010b. Arsenite oxidation by a poorly crystalline manganese-oxide. 2. Results from X-ray absorption spectroscopy and X-ray diffraction. *Environ. Sci. Technol.* 44, 8467-8472. <https://doi.org/10.1021/es102016c>.

326 Manceau, A., Silvester, E., Bartoli, C., Lanson, B., Drits Victor, A., 1997. Structural mechanism of Co^{2+}
 327 oxidation by the phyllomanganate buserite. *Am. Mineral.* 82, 1150–1175. [https://doi.org/10.2138/am-1997-](https://doi.org/10.2138/am-1997-11-1213)
 328 11-1213.

329

330 Manning, B.A., Fendorf, S.E., Bostick, B., Suarez, D.L., 2002. Arsenic(III) oxidation and Arsenic(V)
 331 adsorption reactions on synthetic birnessite. *Environ. Sci. Technol.* 36, 976-981.
 332 <https://doi.org/10.1021/es0110170>.

333

334 Murphy, J., Riley, J.P., 1962. A modified single solution method for the determination of phosphate in
 335 natural waters. *Anal. Chim. Acta* 27, 31-36. [https://doi.org/10.1016/S0003-2670\(00\)88444-5](https://doi.org/10.1016/S0003-2670(00)88444-5).

336

337 Murray, J.W., Dillard, J.G., Giovanoli, R., Moers, H., Stumm, W., 1985. Oxidation of Mn(II)-initial
 338 mineralogy, oxidation-state and aging. *Geochim. Cosmochim. Acta* 49, 463-470.
 339 [https://doi.org/10.1016/0016-7037\(85\)90038-9](https://doi.org/10.1016/0016-7037(85)90038-9).

340

341 Nesbitt, H.W., Canning, G.W., Bancroft, G.M., 1998. XPS study of reductive dissolution of 7Å-birnessite
 342 by H_3AsO_3 , with constraints on reaction mechanism. *Geochim. Cosmochim. Acta* 62, 2097-2110.
 343 [https://doi.org/10.1016/S0016-7037\(98\)00146-X](https://doi.org/10.1016/S0016-7037(98)00146-X).

344

345 Okibe, N., Fukano, Y., 2019. Bioremediation of highly toxic arsenic via carbon-fiber assisted indirect
 346 As(III) oxidation by moderately thermophilic, acidophilic Fe-oxidizing bacteria. *Biotech. Lett.* 41, 1403–
 347 1413. <https://doi.org/10.1007/s10529-019-02746-7>.

348

349 Okibe, N., Koga, M., Morishita, S., Tanaka, M., Heguri, S., Asano, S., Sasaki, K., Hirajima, T., 2014.
 350 Microbial formation of crystalline scorodite for treatment of As(III)-bearing copper refinery process
 351 solution using *Acidianus brierleyi*. *Hydrometallurgy* 143, 34-41.
 352 <https://doi.org/10.1016/j.hydromet.2014.01.008>.

353

354 Oscarson, D.W., Huang, P.M., Liaw, W.K., Hammer, U.T., 1983. Kinetics of oxidation of arsenite by
 355 various manganese dioxides. *Soil Sci. Soc. Am. J.* 47, 644-648.
 356 <https://doi.org/10.2136/sssaj1983.03615995004700040007x>.

357

358 Parikh, S.J., Lafferty, B.J., Meade, T.G., Sparks, D.L., 2010. Evaluating environmental influences on AsIII
 359 oxidation kinetics by a poorly crystalline Mn-oxide. *Environ. Sci. Technol.* 44, 3772-3778.
 360 <https://doi.org/10.1021/es903408g>.

361

362 Sadiq, M., 1997. Arsenic chemistry in soils: An overview of thermodynamic predictions and field
 363 observations. *Water Air Soil Pollut.* 93, 117-136. <https://doi.org/10.1007/bf02404751>.

364

365 Schacht, L., Ginder-Vogel, M., 2018. Arsenite depletion by manganese oxides: A case study on the
 366 limitations of observed first order rate constants. *Soil Syst.* 2, 39.
 367 <https://doi.org/10.3390/soilsystems2030039>.

368

369 Scott, M.J., Morgan, J.J., 1995. Reactions at oxide surfaces. 1. Oxidation of As(III) by synthetic birnessite.
 370 *Enviro. Sci. Technol.* 29, 1898-1905. <https://doi.org/10.1021/es00008a006>.

371

372 Singh, R., Singh, S., Parihar, P., Singh, V.P., Prasad, S.M., 2015. Arsenic contamination, consequences and
 373 remediation techniques: A review. *Ecotoxicol. Environ. Saf.* 112, 247-270.
 374 <https://doi.org/10.1016/j.ecoenv.2014.10.009>.

375

376 Sorlini, S., Gialdini, F., 2010. Conventional oxidation treatments for the removal of arsenic with chlorine
 377 dioxide, hypochlorite, potassium permanganate and monochloramine. *Water Res.* 44, 5653-5659.
 378 <https://doi.org/10.1016/j.watres.2010.06.032>.

379

380 Takashima, T., Hashimoto, K., Nakamura, R., 2012. Mechanisms of pH-dependent activity for water
381 oxidation to molecular oxygen by MnO₂ electrocatalysts. J. Am. Chem. Soc. 134, 1519-1527.
382 <https://doi.org/10.1021/ja206511w>.

383

384 Tanaka, M., Okibe, N., 2018. Factors to enable crystallization of environmentally stable bioscorodite from
385 dilute As(III)-contaminated waters. Minerals 8, 23. <https://doi.org/10.3390/min8010023>.

386

387 Tebo, B.M., Bargar, J.R., Clement, B.G., Dick, G.J., Murray, K.J., Parker, D., Verity, R., Webb, S.M., 2004.
388 Biogenic manganese oxides: properties and mechanisms of formation. Annu. Rev. Earth Planet. Sci. 32,
389 287-328. <https://doi.org/10.1146/annurev.earth.32.101802.120213>.

390

391 Tournassat, C., Charlet, L., Bosbach, D., Manceau, A., 2002. Arsenic(III) oxidation by birnessite and
392 precipitation of manganese(II) arsenate. Environ. Sci. Technol. 36, 493-500.
393 <https://doi.org/10.1021/es0109500>.

394

395 Watanabe, J., Tani, Y., Chang, J., Miyata, N., Naitou, H., Seyama, H., 2013. As(III) oxidation kinetics of
396 biogenic manganese oxides formed by *Acremonium strictum* strain KR21-2. Chem. Geol. 347, 227-232.
397 <https://doi.org/10.1016/j.chemgeo.2013.03.012>.

Figure legends

Fig. 1. Oxidation of As(III) to As(V) coupled with the reduction of biogenic birnessite to Mn^{2+} in the cycle batch test: As(III) concentrations (a), total soluble As concentrations (b), total soluble Mn concentrations (c) and Mn loss from birnessite (d) are shown for each cycle. Birnessite was added only once before the 1st-cycle in all cases (at a pulp density of 0.1%). Likewise, active Mn-oxidizing *Pseudomonas* sp. SK3 cells were added only once before the 1st-cycle (at 10^9 cells/mL) (●). Cell-free controls containing only birnessite (×), as well as birnessite-free controls containing only SK3 cells (○) were also prepared in parallel.

Fig. 2. Transition of the Mn species and AOS (average oxidation state) of birnessite during the cycle batch As(III) oxidation test with or without the presence of Mn-oxidizing *Pseudomonas* sp. SK3 cells (shown in Fig. 1): The ratio of Mn^{2+} (white), Mn(III) (grey) and Mn(IV) (black) (left) were calculated from the linear combination fitting result (dotted lines) of Mn K-edge XANES spectra (solid lines) (right). As Mn standards, $\text{Mn}^{II}\text{SO}_4$, $\text{Mn}^{III}_2\text{O}_3$ and $\delta\text{-Mn}^{IV}\text{O}_2$ were used.

Fig. 3. Comparison of As(III)-oxidizing reactivity between $\alpha\text{-Mn}^{IV}\text{O}_2$ (●) and $\text{Mn}^{III}_2\text{O}_3$ (▲) (both are chemical reagents).

Fig. 4. The effect of initial As(III) concentration on chemical/microbial synergistic cycle between As(III) oxidation by birnessite and birnessite regeneration: The initial As(III) concentration was set to 0.2 mM (●), 0.4 mM (○), 0.5 mM (▲) or 0.7 mM (△). Changes in As(III) concentrations (a), total soluble Mn concentrations (b) and the molar ratio of the released Mn^{2+} ions to oxidized As(III) ions (c) are shown. Grey lines in (c) were hand-drawn to show the approximate trend in each condition.

Fig. 5. Schematic diagram of the column reactor setup: Natural zeolite particles supporting biogenic birnessite and active Mn-oxidizing *Pseudomonas* sp. SK3 cells (“bio-zeolite”) were packed in the acryl column. The As(III) concentration in feed water was set to 0.2 mM. PIPES was removed from the feed water from day 27 on.

Fig. 6. Continuous As(III) oxidation in the bio-zeolite column reactor at different HRTs (12, 6, 4 and 2 hours): (a) As(III) oxidation efficiency (●) vs. Mn lost from the bio-zeolite (○). (b) Total soluble As concentrations at the inlet (△) or outlet (▲) of the column.

Fig. 7. Continuous As(III) oxidation in the bio-zeolite column reactor at the fixed HRT of 3 hours. (a) As(III) oxidation efficiency (\times) and As(III) concentrations at the inlet (Δ) or outlet (\blacktriangle). (b) Mn dissolved from birnessite (\blacktriangle) and pH at the inlet (\square) or outlet (\blacksquare).

Supplemental Fig.1. XRD diffraction patterns of biogenic birnessite before (0 hours) and after (72 hours) the cycle batch As(III) oxidation test, with or without the presence of Mn-oxidizing *Pseudomonas* sp. SK3 cells (shown in Fig. 1). \bullet , birnessite (JCDD 43-1456).